The influence of a WEC array on the Romanian coastal environment

SORIN DIACONU, EUGEN RUSU
Department of Applied Mechanics
Dunarea de Jos University of Galati
Str. Domneasca, Nr. 111, 800201, Galati
ROMANIA
sorin.diaconu@ugal.ro

Abstract: The main objective of the present work is to evaluate the coastal impact of an WECs composed array of six Wave Dragon devices that would operate in the vicinity of the Romanian near shore area. The target area is chosen from the St. Gheorghe sector based on the fact that this region is characterized by coastal erosion and local sediment transport. An overview of the wave climate of the target area based on historical data analysis and various simulations with SWAN model, considering the most relevant conditions which could be expected in the area targeted is carried out. The study performed in the numerical model analysis is focused on the influence of the farm on the shoreline current circulations and on the variations of the incident wave field which interact with the Wave Dragon farm.

Finally, was observed that in the presence of the farm, a significant influence on the wave field appears near the Wave Dragon devices, but this is gradually decreased until the coastline level, while the long shore current velocities appear to be quite sensitive to its presence.

Key-Words: Black Sea, wave power, WEC, renewable energy, electric power, wave height.

1Introduction

The higher request concerning the implementation on large scale of the renewable energy imposed by the EU directives also implies a substantial enhancement of the renewable energy extraction all over Europe.

Wave energy is abundant and is more predictable than wind or solar energy. Although the amount of energy that can be extracted using wave technologies varies depending on the location and weather conditions, wave energy can be accurately predicted using numerical models within a window of a few days. Wave energy also offers much higher energy densities, allowing devices to extract more power from a smaller volume at consequently lower costs.

Shoreline energy converters have been tested for some years and several successful devices have been installed. Nevertheless, the most exciting developments at present are in extracting renewable energy in the near shore and offshore.

Combined wind-wave projects, also known as hybrids, hold great potential down the line when wave technologies have become more established. At that point, wave production might compensate for the intermittency of the offshore wind, while economies of scale developed from offshore wind could accelerate cost reduction for wave components. Although nowadays discussion of hybrid offshore wind-wave projects is limited more to demonstrations or pilot projects, it is expected that in the near future the synergy between wave and wind energy would be better achieved and hybrid platforms will become fully operational and economically sustainable. Despite a certain degree of uncertainty related to the variability in the wave-wind climate, improvements in the accuracy of evaluating the environmental data in the coastal areas would enhance also the accuracy of the predictions that future energy convertors yield.

The target of the present work is a coastal environment located in the western side of the Black Sea, which is not considered as being an environment rich in wave energy. On the other hand, due to the technological developments as regards harvesting the renewable energy resources, which are expected to be very high in the near future, this area can become interesting especially in relationship with the hybrid projects combining the marine energy from waves, wind, marine currents, thermal gradients, and differences in salinity.

Until now, several evaluations of the wave conditions and of the wave energy resources in the

Black Sea have been made and among these may be the most relevant is that of Rusu [1] where it has been proved that the western side of the sea is its most energetic part. Also, others studies that were carried out focused on this region are those of Rusu [2], Rusu and Ivan [3] and Rusu and Macuta [4] where the presence of various hot spots from the point of view of the wave energy has been identified. These hot spots are areas near the coast where significant differences in terms of wave conditions usually appear.

In relationship with the wind energy resources in the area targeted, Onea and Rusu [5] analyzed the variability and wind conditions in the western side of the Black Sea, which has been found to have similar energetic features with the Northern and the Baltic seas, where the wind energy in the coastal environment is now intensively extracted.

Harvesting the wave energy and transform it in electricity implies wave energy convertors (WEC) that transform in the first stage the wave energy in mechanical energy, and then this is again transformed in electricity. Several types of devices as well as an overview on the WEC evolution are given in Babarit [6]. Sea waves generate high forces at low velocities and the hydraulic systems seem to be the most appropriate to absorb the energy in such conditions. The device is fixed at a location with a mooring system. The electricity is transmitted to the sea bottom through a flexible cable and afterwards to the coast by a cable line. The waves depend on the characteristics of the wind that generates them and in general the energetic conditions are significantly higher in winter time than in summer time.

On the other hand, the implementation of the energy farms is related with a correct evaluation of their impact on coastline dynamics, because changes might appear in relationship with the energy and the direction of the waves as they propagate from the energy farm further towards the coast. The environmental impacts of the wave energy farms are yet insufficiently studied. Although this impact should not be expected as necessarily negative, since reducing the wave energy might produce benefits in several coastal areas, to evaluate the sensitivity of the nearshore wave climate to the extraction of the renewable energy still represents a very important issue and a lot of work should be done in this direction.

In this context, the objective of the present work is to evaluate the coastal impact of a WEC array composed of six Wave Dragon devices disposed in one line that would operate in the west side of Black Sea. Some other studies are those of Millar [7] for the Wave Hub project or by Palha [8] that study the effect Pelamis wave farm on the shoreline wave climate which is situated close to the Portuguese coast and also by Ponce de Leon [9] that studied the influence of a wind farm in the near shore. The impact on the coastal dynamics is dependent both on the bathymetric features and on the particularities of the environmental matrix. For this reason, extended evaluations should be carried out in each coastal environment where a new structure or energy farm will be installed. These especially concern the medium and long term changes induced in the shoreline wave climate and dynamics.

From this perspective, the present study might represent a step forward to the investigation on the potential impact of the implementation of large scale wave energy arrays by providing some insight in relationship with the influence of a Wave Dragon based farm that would operate in the coastal environment. The present target area is located in the western side of the Black Sea close to the mouths of the Danube River, and this was found by Rusu [10] as being one of the most energetic parts of the western side of the sea. Moreover, the results of the present work can be easily extrapolated to many other coastal environments.

2Theoretical background of the numerical models considered

Since a deterministic approach of the sea waves is in general not feasible, the most adequate representation of the waves is based on the spectral concept. The wave spectrum represents the Fourier transform of the autocorrelation function of the free surface elevation. The spectral wave model considered in the present study is SWAN (Simulating Waves Near shore, Booij [11]). This is considered the state-of-the art phase averaged shallow water wave model and solves the wave action density balance equation which can be expressed as:

$$\frac{\partial}{\partial t}N+\frac{\partial}{\partial x}C_{gx}N+\frac{\partial}{\partial y}C_{gy}N+$$
$$+\frac{\partial}{\partial \sigma}C_{\sigma}N+\frac{\partial}{\partial \theta}C_{\theta}N=\frac{S}{\sigma} \quad (1)$$

where N is the wave action density, C_{gx}, C_{gy}, C_{σ}, and C_{θ} represent the propagation speeds in the geographical space (x, y) in the frequency space (σ) and in the directional space (θ), respectively. S/σ represents source and sink terms that account in deep water for processes as wave generation by wind, white capping dissipation and non linear wave-wave interactions (quadruplets). In shallow water, additional processes as bottom friction, depth induced breaking and triad wave-wave interactions are also introduced. The model can be now utilized with either Cartesian or spherical

coordinates, it has a parameterization to counteract the garden-sprinkler-effect, which is characteristic to large areas and also includes a phase-decoupled diffraction approximation.

A lot of phenomena are generated from the dissipation in the surf zone by breaking, but for a practical application, the generation of the long shore currents is most significant, obtaining considerable strength and being a significant factor in controlling the morphology of the beaches. They can also have impacts on human activities in the coastal zone. Calculation of the current velocity is usually based on radiation stress theory (Longuet-Higgins [12]) and various 1D, 2D, and 3D numerical models have been developed to predict these currents. A widely known general prediction system for near shore circulation is SHORECIRC (Svendsen [13]). This is a quasi-3D model that combines a numerical solution for the depth-integrated 2D horizontal momentum balance equations with an analytical solution for the 3D current profiles. The restrictions of the model are very mild and the basic circulation equations solved can therefore in general be considered very accurate. In addition, such a model catches the non-linear feedback between wave generated currents and the waves that generate them. Nevertheless the model works in the time domain and is quite expensive in terms of computational resources. A simpler, but considerably faster, model is Surf, or Navy Standard Surf Model (NSSM), (Mettlach [14]). This is a parametric one-dimensional model that estimates the wave induced long shore currents by solving the following equation for the long shore current:

$$\tau_y^r + \rho \frac{\partial}{\partial x}\left[\mu h \frac{\partial V}{\partial x}\right] - \langle \tau_y^b \rangle + \tau_y^w = 0 \qquad (2)$$

The first term in this equation, τ^r_y, represents the long shore directed radiation stress due to the incident waves, the second term represents the horizontal mixing term due to cross-shore gradients in the long shore current velocity V, the third term, τ^b_y, is the wave averaged bottom stress and the last term, τ^w_y, represents the long shore wind stress. The model includes a parametric relation for cross-shore growth and dissipation of waves due to breaking and additional relations are included for estimating percent breaking, the number of lines of breakers and breaker type. Because NSSM is one-dimensional several assumptions are utilized. In particular, the bottom contours are considered straight and parallel, the currents depth-uniform and directional wave spectra narrow-banded in frequency and direction.

Evaluations in the Italian near shore of the waves and near shore currents were performed by Conley and Rusu [15], [16] with SWAN and NSSM models and their results proved that this approach can be considered reliable for a wide range of coastal applications. In order to increase the properties of the two models and for simplicity and reliability, Rusu [17] joined the two models in a user friendly computational tool named as the "Interface for SWAN and Surf Models" (ISSM). The utility of this computational environment have been showed by Rusu and Guedes Soares [18] with validations against in situ measurements and comparisons with the SHORECIRC modeling system performed in the Portuguese near shore. This modeling system will be also used in the present work.

The computational domain is illustrated in Fig. 5. This is a rectangle with about 17.5km in *x*-direction (cross shore) and 20km in *y*-direction (long shore). The main characteristics and physical processes activated are presented in Table 1. In this table Δx and Δy represent the resolution in the geographical space, $\Delta\theta$ is the resolution in the directional space, *nf* is the number of frequencies in the spectral space, $n\theta$ is the number of directions in the spectral space, *ngx* is the number of the grid points in *x*-direction, *ngy* is the number of grid points in *y*-direction and *np* is the total number of grid points.

Some details will be given next in relationship with the implementation of the modeling conditions in the target area. The input fields considered are also indicated in Table 1 as follows: *wave* represents the wave forcing, *tide* is the tide forcing, *wind* represents the wind forcing, *crt* is the current field. The physical processes activated are coded as: *gen* is the generation by wind, *wcap* indicates the white capping process, *quad* represents the quadruplet nonlinear interactions, *triad* indicates the activation of the triad nonlinear interactions, *diff* is the diffraction process (phase decoupled), *bfric* represents the bottom friction, *set up* is the wave induced set up and *br* indicates the activation of the depth induced wave breaking.

3 Main particularities of the WEC and of the wave conditions in the target area

The WEC considered in the present work is the Wave Dragon (Kofoed [19]).The basic idea of this wave energy converter device is to use well-known and well-proven principles from traditional hydro power plants in an offshore floating platform of the overtopping type. The device elevates waves to a reservoir where water is passing through a number of turbines and in this way transformed into electricity. This is a typical terminator type WEC, for which the conservative

approach is to assume that the devices will absorb all suitable surfing wave energy across the full width of the reservoir.

Table 1: Characteristics of the computational domain defined for the SWAN simulations and the physical parameterizations activated

SWAN model	**Coordinates**	**Δx × Δy (m)**	**Δθ (°)**	**Mode/ scheme**	**nf**	**nθ**	***ngx* × *ngy* = *np***
	Cartesian	50 × 50	5	stat/ BSBT	34	35	355×406=144130

Input / Process	**wave**	**wind**	**tide**	**crt**	**gen**	**wcap**	**quad**	**triad**	**diffr**	**bfric**	**set up**	**br**
SWAN	X	X	0	X	X	0	X	X	X	X	X	X

The Wave Dragon (Fig. 4) consists of two wave reflectors that direct the waves towards a curved ramp which overtops in a water reservoir and therefore has an increased potential energy compared to the surrounding sea. Thus the Wave Dragon directly utilizes the energy of the water's motion.

To reduce rolling and keep the platform stable, the Wave Dragon must be large and heavy, having only one kind of moving parts: the turbines. This makes him to be a durable and resistant structure. This is essential for any device bound for operations offshore, where extreme conditions and fouling, seriously affect any moving parts. If the waves do not interact with the ramp they are reflected under his structure or diffracted away. Also, to improve the device performances, two reflectors are placed, hinged to the platform, which reflect the waves towards the ramp. The experiments showed that the ramp must to be short to reduce the loss of energy and due the elliptical form the overtopping increases significantly.

The device has a very complex design because it must be a perfect relationship between ramp, wave reflectors, wave height, the floating height of the device and the amount of water overtopping and storing in the reservoir (Fig. 4b). The components are all well established technologies and the Wave Dragon is a particular application combining these to produce electricity from the waves.

The target area considered in the present study was found to be among the most energetic sites from the western side of the Black Sea (Rusu [1], [10]) and is located at the south of Sulina channel, which is also a very important navigation sector since represents the main gate in the seventh Trans European transportation corridor (Fig. 1). It has to be highlighted also that in this region the wave fields are characterized by significant variations during the year.

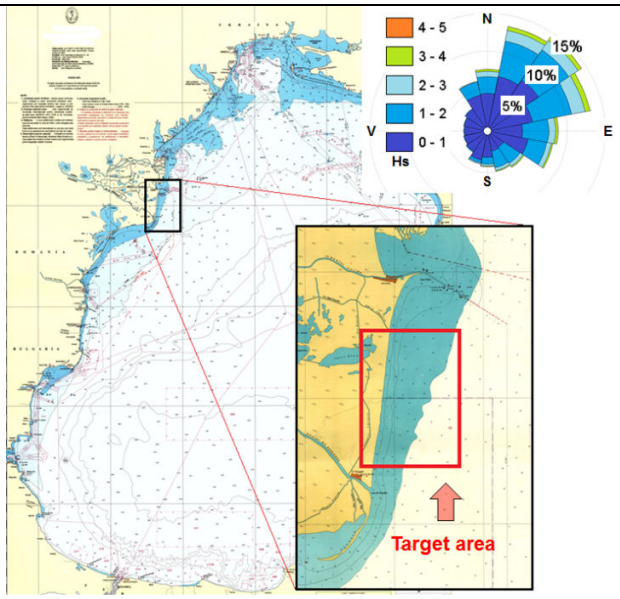

Fig. 1: Location of the target area and the wave conditions resulting from an analysis of 5 year of data (2006-2011).

The wave data analysis presented in this section considered data measured at a buoy which operated in the western sector of the Black Sea close to the target area. The measurements were made daily in the five-year time interval 2006 and 2011. The results were structured for total and winter time, respectively. In this work winter time represents the time interval between October to March. Fig. 1 shows together with the target area the directional distributions of the H_s classes as reflected by the buoy measurements. It can be observed that the lowest wave heights correspond to the western direction because of the presence of the coast in that side while the dominant wave direction is from the northeastern side. It can be also seen that from the same direction higher waves are usually coming in

comparison with other directions. In Fig. 2, the *Hs* classes are presented in percents in terms of the number of occurrences, illustrating in parallel the results for total time (a) and wintertime (b), respectively. The monthly maximum values of the significant wave heights and mean wave periods are shown in Fig. 3.

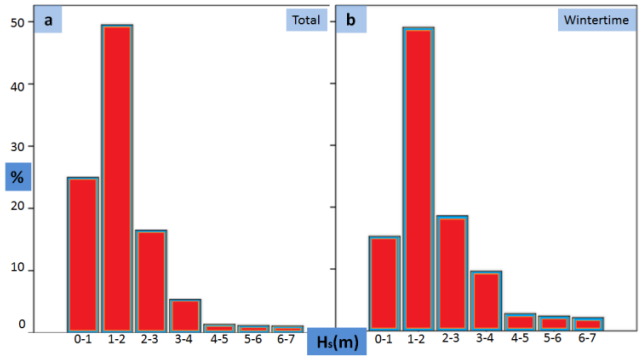

Fig. 2: Analysis of the wave data measured at buoy close to the target area in the period 2006-2011: a) Classes of significant wave height (*Hs)* for total time interval; b) *Hs* classes for wintertime.

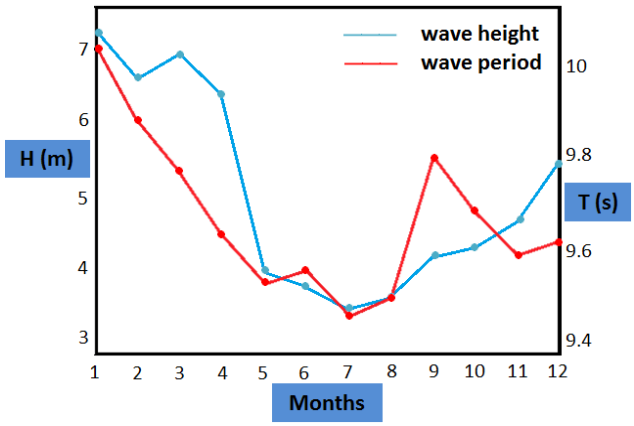

Fig. 3: Analysis of the wave data measured at a buoy close to the target area in the period 2006-2011: H(m) monthly maximum wave height; T(s) monthly maximum wave period.

The results show that the highest probability of occurring waves with significant heights, greater than 7m is in the time interval between December and January. This possibility begins in September and lasts until the end of March. The same evolution can be seen for the significant wave heights in the classes 4-5m, 5–6m and 6–7m.Waves with significant wave heights in the range 1-2m are present in a considerable proportion all over the year, with a minimum in March and a maximum in July. For the waves smaller than 1m, the frequency of occurrence in summertime is almost double than in wintertime. The highest value of the significant wave is 7.08m and corresponds to waves coming from the northeastern direction. As regards the wave periods, there are not so relevant differences between winter and total time.

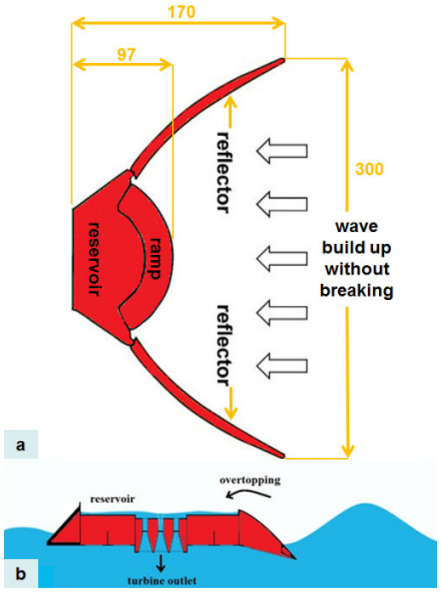

Fig. 4: a) Main structural elements of a Wave Dragon WEC in plan view - dimensions in meters; b) cross sectional view of the reservoir part of the Wave Dragon.

4 Model simulations and discussion of the results

As the attenuator type devices, the terminator devices have the length equal to or greater than the wavelength. The efficiency of these devices is directionally dependent, that is they must weathervane relatively to the wave propagation. Simulations with the SWAN model have been performed for various cases that reflect better the most relevant wave patterns in the target area.

For accounting in the wave model on the Wave Dragon array geometry, the command obstacle that is available in SWAN was considered.The obstacle is sub-grid in the sense that it is narrow compared to the spatial meshes but its length should be at least one mesh length. The location of the obstacle is defined by a sequence of corner points of a line. The obstacles interrupt the propagation of the waves from one grid point to the next. Such an obstacle will affect the wave field in three ways: it will reduce the wave height of waves propagating through or over the obstacle all along its length, it will cause waves to be reflected, and it will cause diffraction around its end. Therefore the model can reasonably account for waves around an

ISBN: 978-1-61804-195-1

obstacle if the directional spectrum of incoming waves is not too narrow. There are several mechanisms for transmission of waves. In SWAN, this can be computed as transmission of waves passing over a dam with a closed surface or as a constant transmission coefficient which was the choice in the present work. Together with the command obstacle, either specular reflection, when the angle of reflection equals the angle of incidence, or diffuse reflection, where incident waves are scattered over reflected direction, may be considered. In this way the effect on the waves in front of the wave arrays might be also accounted for. To accommodate diffraction in SWAN simulations, a phase-decoupled refraction-diffraction approximation is implemented. It is expressed in terms of the directional turning rate of the individual wave components in the 2D wave spectrum. The approximation is based on the mild-slope equation for refraction and diffraction, omitting phase information. It does therefore not permit coherent wave fields in the computational domain. According to the technical data of the Wave Dragon device the transmission coefficient was set to 0.68 and the diffuse reflection coefficient to 0.2.

4.1 Evaluations in the geographical and in the spectral spaces

An in depth analysis of the wave conditions has been performed. These correspond to two different situations that were considered in the present study, WD0 (without any device operating in the target area) and WD6 (with six Wave Dragon devices operating in line in the target area).

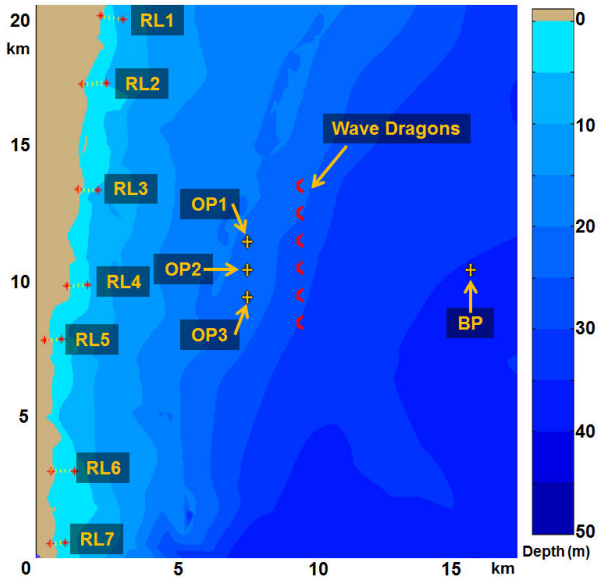

Fig. 5: The computational domain considered for the simulations with numerical models. In background the bathymetry is represented while in foreground the Wave Dragon, the reference points and the reference lines. BP indicates the boundary point, OP are the offshore points and RL represent the reference lines considered for the analysis of the near shore currents. Each offshore extremity point of the above reference lines is denoted as NP (near shore point).

In Fig. 5, some reference points are illustrated, the first reference point is denoted as BP and indicates the boundary point and three other reference points are defined at 1.8km down wave from the WD farm and they have been denoted as offshore points (OP). Moreover, in order to assess the coastal impact of the wave farm by evaluating the wave induced near shore currents, seven reference lines (RL) were positioned along the entire coast and they are denoted as RL1 to RL7. The extremities of each reference line from the offshore side denoted as NP (near shore point) and these points were taken into consideration for analyzing in both geographical and spectral spaces the near shore waves.

In Fig.6 and 7is presented the impact in the geographical space on the wave field of a wave farm based on Wave Dragon devices for two different case studies: CS1 (*Hs*=1m, *Tm*=3s, *Dir*=90°) and CS2 (*Hs*=3m, *Tm*=6s, *Dir*=90°).

ISBN: 978-1-61804-195-1

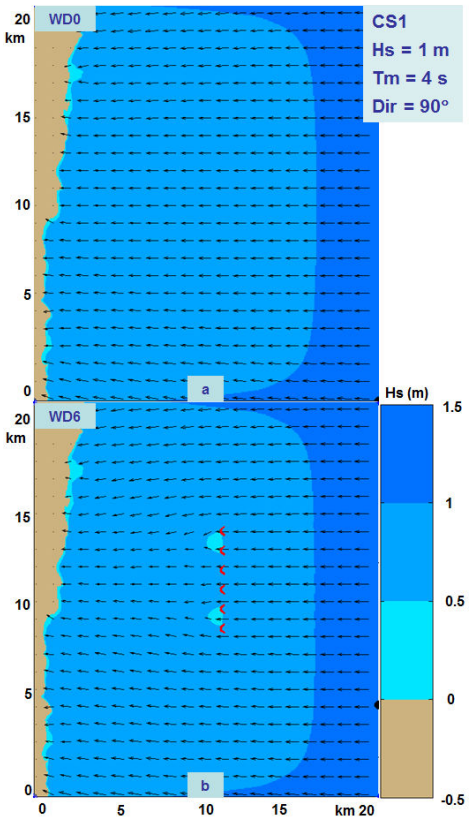

Fig. 6: Evaluation in the geographical space of the impact on the wave field of a wave farm based on Wave Dragon WECs that operates in the target area. CS1 – average to high energetic conditions and waves coming from east (90° in nautical convention). a) SWAN simulation for the case without Wave Dragons (WD0). b) SWAN simulation for the case when six Wave Dragons operate in line (WD6). The *Hs* scalar fields are presented in background while in foreground the wave vectors are indicated.

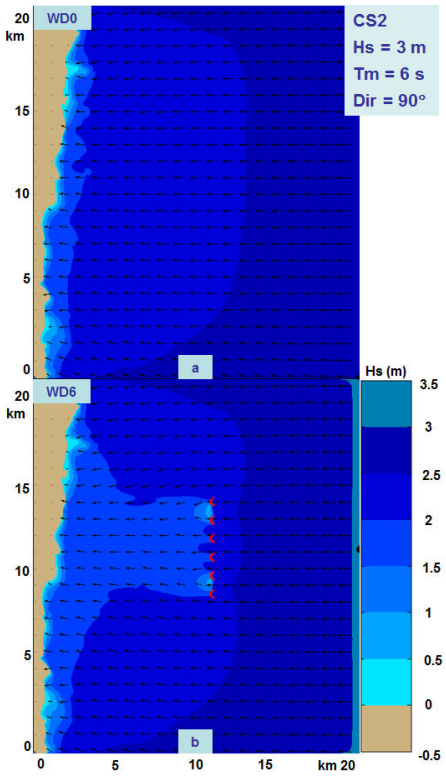

Fig. 7: Evaluation in the geographical space of the impact on the wave field of a wave farm based on Wave Dragon WECs that operates in the target area. CS2 – high energetic conditions and waves coming from east (90° in nautical convention). a) SWAN simulation for the case WD0. b) SWAN simulation for the case WD6. The Hs scalar fields are presented in background while in foreground the wave vectors are indicated.

These cases were chosen because it has been observed that they present the highest differences between the two situations: with and without the energy farm. Thus, at the same time there are presented in the figure the two situations which where considered, without any device deployed in the target area (WD0) and when six Wave Dragon devices operate in line (WD6), respectively.

It can be seen in the two figures mentioned above that for CS1 that corresponds to average wave conditions the impact is visible only locally the wave field, being attenuated after about 0.5km down wave while as the wave heights increase, the impact propagates further towards the coast, like in CS2.

ISBN: 978-1-61804-195-1

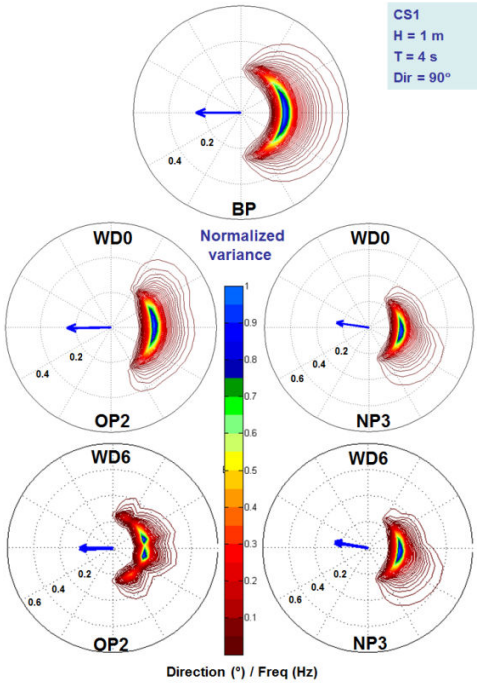

Fig. 8: Evaluation in the spectral space of the impact on the wave field of a wave farm based on Wave Dragon WECs that operates in the target area for CS1. a) BP for WD0. b) OP2 for WD0. c) NP3 for WD0, d) OP2 for WD6, e) NP3 for WD6.

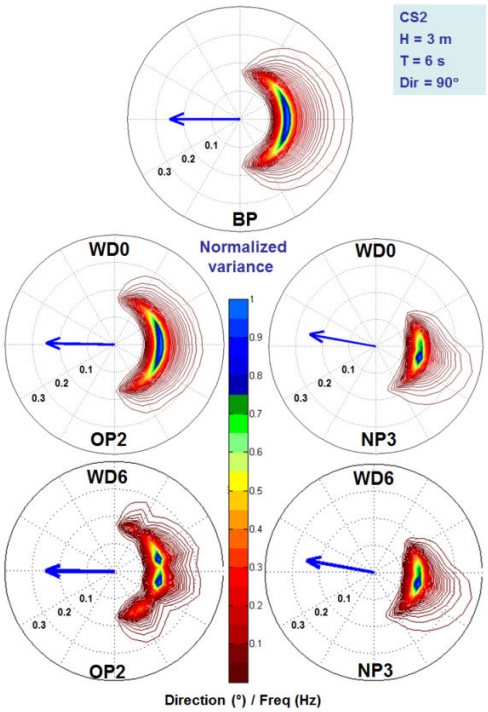

Fig. 9: Evaluation in the spectral space of the impact on the wave field of a wave farm based on Wave Dragon WECs that operates in the target area for CS2. a) BP for WD0. b) OP2 for WD0. c) NP3 for WD0, d) OP2 for WD6, e) NP3 for WD6.

The evaluation in the spectral space of the Wave Dragon energy farm impact is illustrated in Fig. 8 and 9 for the same two case studies (CS1 and CS2), where the 2D wave spectra were analyzed in parallel in the reference points OP2 and NP3 for the two different configurations considered (WD0, and WD6). In this figure a JONSWAP type spectrum was considered.

The boundary point (BP) presents the wave conditions unaffected in any way by presence of the wave farm. Due to the presence of the Wave Dragons, the single peak JONSWAP spectrum is transformed in a double peak spectrum immediately after the WEC array (as for example in OP2) but this spectral shape does not propagate further in the geographical space and at the level of the near shore (the reference point NP3) no significant difference occurs in terms of the spectral shapes between the two different configurations considered (WD0 and WD6).

In Table 2 and in Table 3 a detailed data representation of the wave variation is given for CS1 and CS2, respectively. This representing the values of the wave parameters in all the reference points defined (BP, OP1, OP2, OP3, NP1, NP2, NP3, NP4, NP5, NP6 and NP7) for the two configurations considered (WD0 and WD6).

ISBN: 978-1-61804-195-1

Table 2: CS1 (*Hs*=1m, *Tm*=4s, *Dir*=90°), evaluation of the impact of the energy farms on the waves in the reference points OP1 (northern offshore point), OP2 (central offshore point), OP3 (southern offshore point), and in the point NP1-NP7. WD0 – no energy converter, WD6 – four Wave Dragon energy converters operating in line.

	WD	Hs (m)	Emax (m^2/Hz/deg)	Dir (deg)	DSPR (deg)	Tm/Tp (s)	Wlen (m)	Px (m^3/s)	Py (m^3/s)	Fx (N/m^2)	Fy (N/m^2)
BP	0	0.9	0.40	90.0	32.48	3.5/4	18.5	-0.13	0.00	-0.01	-0.00
	6	0.9	0.40	90.0	33.18	3.5/4	18.5	-0.13	-0.00	-0.01	-0.00
OP1	0	0.8	0.35	89.6	33.25	3.7/4	20.7	-0.10	-0.00	-0.00	-0.00
	6	0.7	0.32	91.4	33.57	3.7/4	20.4	-0.07	0.00	-0.00	0.00
OP2	0	0.8	0.31	90.0	33.23	3.7/4	20.7	-0.10	0.00	-0.00	-0.00
	6	0.7	0.31	89.3	33.81	3.7/4	20.5	-0.07	-0.00	-0.00	-0.00
OP3	0	0.8	0.35	90.4	33.23	3.7/4	20.7	-0.10	0.00	-0.00	-0.00
	6	0.6	0.30	93.1	38.28	3.7/4	20.6	-0.06	0.00	-0.00	0.00
NP1	0	0.8	0.34	80.4	30.00	3.5/4	17.1	-0.11	-0.02	0.13	0.03
	6	0.8	0.50	78.6	29.04	3.5/4	16.9	-0.11	-0.02	0.13	0.03
NP2	0	0.7	0.31	89.3	25.78	3.6/4	17.9	-0.09	-0.00	0.16	0.04
	6	0.6	0.32	86.2	26.05	3.6/4	17.6	-0.08	-0.00	0.14	0.03
NP3	0	0.7	0.34	98.8	25.54	3.5/4	15.1	-0.10	0.01	0.07	0.23
	6	0.7	0.34	99.8	24.95	3.5/4	15.0	-0.09	0.01	0.07	0.22
NP4	0	0.7	0.33	89.8	25.90	3.6/4	17.1	-0.09	-0.00	0.22	0.04
	6	0.6	0.28	90.3	27.85	3.6/4	16.8	-0.08	0.00	0.19	0.03
NP5	0	0.7	0.29	95.3	25.44	3.6/4	17.8	-0.08	0.01	0.14	-0.01
	6	0.6	0.29	98.3	26.13	3.6/4	17.5	-0.07	0.01	0.13	-0.00
NP6	0	0.7	0.29	85.4	25.90	3.6/4	17.3	-0.08	-0.01	-0.01	0.01
	6	0.6	0.29	87.3	25.60	3.6/4	17.1	-0.08	-0.01	-0.01	0.01
NP7	0	0.7	0.34	98.8	25.54	3.5/4	15.1	-0.10	0.01	0.07	0.23
	6	0.7	0.34	99.8	24.95	3.4/4	15.0	-0.09	0.01	0.07	0.22

ISBN: 978-1-61804-195-1

Table 3:CS2 (*Hs*=3m, *Tm*=6s, *Dir*=90°),evaluation of the impact of the energy farms on the waves in the reference points OP1, OP2, OP3, NP1-NP7.

	WD	Hs (m)	Emax (m^2/Hz /deg)	Dir (deg)	DSPR (deg)	Tm/Tp (s)	Wlen (m)	Px (m^3/s)	Py (m^3/s)	Fx (N/m^2)	Fy (N/m^2)
BP	0	2.7	5.27	90.0	32.28	5.4/6	42.7	-1.74	0.00	-0.10	-0.00
	6	2.7	5.27	90.0	32.94	5.4/6	42.7	-1.73	0.00	-0.10	-0.00
OP1	0	2.3	4.31	90.5	32.44	5.6/6	46.2	-1.38	0.02	0.04	-0.01
	6	1.9	3.81	92.2	32.67	5.5/6	45.6	-0.88	0.04	0.04	0.01
OP2	0	2.4	4.31	91.0	32.39	5.6/6	46.4	-1.38	0.03	0.03	-0.01
	6	1.9	3.70	90.3	33.00	5.5/6	45.8	-0.87	0.01	0.03	-0.00
OP3	0	2.4	4.32	91.5	32.43	5.6/6	46.5	-1.38	0.04	0.02	-0.03
	6	1.8	3.64	94.3	37.56	5.6/6	46.1	-0.74	0.06	0.04	-0.02
NP1	0	2.2	4.92	78.9	26.10	5.5/6	33.6	-1.31	-0.25	-0.77	-0.60
	6	2.2	5.02	77.2	25.23	5.5/6	33.4	-1.29	-0.29	-0.64	-0.55
NP2	0	1.8	4.55	89.2	19.58	5.6/6	33.1	-0.96	-0.01	0.06	0.23
	6	1.7	4.60	86.5	19.64	5.6/6	32.9	-0.85	-0.05	0.50	0.30
NP3	0	1.5	3.08	100.1	20.07	5.4/6	28.4	-0.56	0.10	-1.48	0.45
	6	1.5	3.10	100.4	19.81	5.4/6	28.4	-0.56	0.10	-1.47	0.46
NP4	0	1.6	3.90	93.9	18.68	5.6/6	29.4	-0.69	0.04	-3.26	-0.05
	6	1.5	3.15	93.8	20.22	5.6/6	29.2	-0.64	0.04	-2.54	-0.08
NP5	0	1.7	3.46	95.0	19.98	5.6/6	31.6	-0.79	0.06	-0.24	-0.14
	6	1.6	3.51	96.9	20.23	5.5/6	31.4	-0.72	0.08	0.18	0.00
NP6	0	1.7	3.63	83.6	18.51	5.6/6	31.8	-0.79	-0.10	-0.98	-0.31
	6	1.6	3.74	84.5	18.20	5.6/6	31.7	-0.78	-0.08	-0.89	-0.25
NP7	0	1.5	3.08	100.1	20.07	5.4/6	28.4	-0.56	0.10	-1.48	0.45
	6	1.5	3.10	100.4	19.81	5.4/6	28.4	-0.56	0.10	-1.47	0.46

Some other relevant situations are presented in Tables 4-10, this time the analysis being focused only on the offshore points (OP1, OP2 and OP3) where the influence of the wave energy farm is in fact really relevant for the two situation mentioned above. The parameters considered in Tables 2-10 are significant wave height (*Hs*), maximum variance (*Emax*), mean wave direction (*Dir*),directional spreading(DSPR), peak period (*Tp*), mean period (*Tm*), wave length (*Wlen*), the components of the energy transport (*Px, Py*) and the components of the wave forces (*Fx, Fy*).

The results presented in the above tables show again that indeed relevant differences occur at the offshore reference points that were defined while as regards the near shore point NP1-NP7 these differences are significantly attenuated.

4.2 Assessment of the impact on the shoreline dynamics

Various phenomena are generated by the energy dissipation in the coastal environment and the most relevant are the near shore currents because they contribute to the sediment transport affecting directly the coastal dynamics. It is thus very important to find out how an energy farm will affect the near shore circulation patterns by his presence in the marine environment and to estimate which will be the medium to long term impact on the coastal dynamics of the energy farm.

The near shore currents were evaluated along the reference lines RL1-RL7, for the two different configurations considered (WD0 and WD6). The results concerning the maximum long shore current velocity are presented in Tables 11, 12 and 13. Table 11 presents the results corresponding to *Hs*=1m at three different wave directions (30°, 90°,150°) while Tables 12 and 13 for *Hs*=3m and *Hs*=5m, respectively, with the same wave directions (30°, 90°,150°).

Table 4: Evaluation of impact of the energy farms on the waves in the reference points OP1, OP2 and OP3 for the wave conditions *Hs*=1m, *Tm*=4s, *Dir*=30°.

	WD	Hs (m)	Emax (m^2/Hz /deg)	Dir (deg)	DSPR (deg)	Tp/Tm (s)	Wlen (m)	Px (m^3/s)	Py (m^3/s)	Fx (N/m^2)	Fy (N/m^2)
BP	0	0.8	0.39	34.1	32.76	3.6/4	19.1	-0.06	-0.10	-0.00	-0.01
	6	0.8	0.40	33.9	33.10	3.6/4	19.1	-0.06	-0.10	-0.00	-0.01
OP1	0	0.8	0.35	32.2	31.52	3.7/4	20.4	-0.05	-0.09	-0.00	-0.00
	6	0.7	0.36	24.1	31.75	3.6/4	20.1	-0.03	-0.07	-0.00	-0.00
OP2	0	0.8	0.35	33.1	31.29	3.7/4	20.5	-0.05	-0.08	-0.00	-0.00
	6	0.7	0.35	27.2	32.50	3.6/4	20.2	-0.03	-0.07	-0.00	-0.00
OP3	0	0.8	0.34	34.2	30.93	3.7/4	20.6	-0.05	-0.08	-0.00	-0.00
	6	0.7	0.34	26.4	30.07	3.6/4	20.3	-0.03	-0.06	-0.00	-0.00

Table 5: Evaluation of impact of the energy farms on the waves in the reference points OP1, OP2 and OP3 for the wave conditions *Hs*=1m, *Tm*=4s, *Dir*=150°.

	WD	Hs (m)	Emax (m^2/Hz /deg)	Dir (deg)	DSPR (deg)	Tm/Tp (s)	Wlen (m)	Px (m^3/s)	Py (m^3/s)	Fx (N/m^2)	Fy (N/m^2)
BP	0	0.8	0.39	145.6	32.69	3.6/4	19.1	-0.06	0.10	-0.00	0.01
	6	0.8	0.39	145.8	33.07	3.6/4	19.1	-0.06	0.10	-0.00	0.01
OP1	0	0.8	0.34	146.3	31.50	3.7/4	20.7	-0.05	0.08	-0.00	0.00
	6	0.7	0.33	152.2	32.59	3.7/4	20.4	-0.03	0.07	-0.00	0.00
OP2	0	0.8	0.34	147.1	31.70	3.7/4	20.6	-0.05	0.08	-0.00	0.00
	6	0.7	0.35	155.3	31.63	3.7/4	20.5	-0.03	0.07	0.00	0.00
OP3	0	0.8	0.35	147.9	31.95	3.7/4	20.5	-0.05	0.09	-0.00	0.00
	6	0.7	0.35	157.1	27.94	3.7/4	20.5	-0.03	0.08	-0.00	0.00

Table 6: Evaluation of impact of the energy farms on the waves in the reference points OP1, OP2 and OP3 for the wave conditions *Hs*=3m, *Tm*=6s, *Dir*=30°.

	WD	Hs (m)	Emax (m^2/Hz /deg)	Dir (deg)	DSPR (deg)	Tm/Tp (s)	Wlen (m)	Px (m^3/s)	Py (m^3/s)	Fx (N/m^2)	Fy (N/m^2)
BP	0	2.6	5.12	35.0	32.51	5.4/5.8	43.8	-0.90	-1.30	-0.04	-0.05
	6	2.6	5.12	34.9	32.84	5.4/5.8	43.9	-0.90	-1.30	-0.04	-0.05
OP1	0	2.3	4.24	34.8	30.62	5.5/5.8	45.9	-0.70	-1.10	0.04	-0.04
	6	2.0	4.31	27.0	31.07	5.5/5.8	45.1	-0.40	-0.90	0.05	-0.02
OP2	0	2.2	4.17	36.0	30.24	5.5/5.8	46.0	-0.70	-1.00	0.03	-0.03
	6	1.9	4.12	30.6	31.61	5.5/5.8	45.2	-0.50	-0.80	0.04	-0.01
OP3	0	2.2	4.11	37.2	29.97	5.5/5.8	46.2	-0.70	-1.00	0.03	-0.05
	6	1.9	4.02	29.8	29.15	5.5/5.8	45.4	-0.40	-0.80	0.03	-0.03

ISBN: 978-1-61804-195-1

Table 7: Evaluation of impact of the energy farms on the waves in the reference points OP1, OP2 and OP3 for the wave conditions *Hs*=3m, *Tm*=6s, *Dir*=150°.

	WD	Hs (m)	Emax (m^2/Hz /deg)	Dir (deg)	DSPR (deg)	Tm/Tp (s)	Wlen (m)	Px (m^3/s)	Py (m^3/s)	Fx (N/m^2)	Fy (N/m^2)
BP	0	2.6	5.12	144.6	32.45	5.4/5.8	43.9	-0.90	1.30	-0.04	0.05
	6	2.6	5.11	144.8	32.83	5.4/5.8	43.9	-0.90	1.30	-0.04	0.05
OP1	0	2.2	4.01	143.4	30.12	5.5/5.8	46.1	-0.70	1.00	0.04	0.01
	6	1.9	3.95	148.8	31.38	5.4/5.8	45.5	-0.50	0.80	0.04	0.01
OP2	0	2.2	4.10	144.4	30.49	5.5/5.8	46.1	-0.70	1.00	0.03	0.02
	6	2.0	4.14	152.3	30.67	5.4/5.8	45.6	-0.40	0.80	0.05	0.01
OP3	0	2.3	4.21	145.7	30.79	5.5/5.8	46.0	-0.70	1.10	0.03	0.01
	6	2.0	4.23	154.9	26.79	5.4/5.8	45.9	-0.40	1.00	0.04	0.01

Table 8: Evaluation of impact of the energy farms on the waves in the reference points OP1, OP2 and OP3 for the wave conditions *Hs*=5m, *Tm*=8s, *Dir*=30°.

	WD	Hs (m)	Emax (m^2/Hz /deg)	Dir (deg)	DSPR (deg)	Tm/Tp (s)	Wlen (m)	Px (m^3/s)	Py (m^3/s)	Fx (N/m^2)	Fy (N/m^2)
BP	0	4.5	18.51	34.6	32.15	7.1/8.2	72.9	-3.70	-5.50	-0.08	-0.17
	6	4.5	18.51	34.4	32.52	7.1/8.2	73.0	-3.70	-5.50	-0.08	-0.17
OP1	0	3.9	15.12	39.9	29.34	7.2/8.2	73.2	-3.70	-4.30	0.43	-0.24
	6	3.3	13.65	32.3	30.60	7.2/8.2	72.0	-2.20	-3.40	0.43	-0.10
OP2	0	3.8	15.07	41.0	28.81	7.2/8.2	73.1	-3.60	-4.00	0.36	-0.16
	6	3.3	12.46	36.2	30.66	7.2/8.2	72.1	-2.30	-3.10	0.32	-0.07
OP3	0	3.8	14.97	42.5	28.63	7.2/8.2	73.4	-3.60	-3.80	0.30	-0.27
	6	3.1	11.93	35.5	28.12	7.2/8.2	72.3	-2.10	-2.90	0.25	-0.28

Table 9: Evaluation of impact of the energy farms on the waves in the reference points OP1, OP2 and OP3 for the wave conditions *Hs*=5m, *Tm*=8s, *Dir*=90°.

	WD	Hs (m)	Emax (m^2/Hz /deg)	Dir (deg)	DSPR (deg)	Tm/Tp (s)	Wlen (m)	Px (m^3/s)	Py (m^3/s)	Fx (N/m^2)	Fy (N/m^2)
BP	0	4.7	18.77	90	32.57	7/ 8.2	70.9	-7.20	0.02	-0.20	-0.04
	6	4.7	18.77	90.1	33.25	7/ 8.2	71.0	-7.10	0.02	-0.20	-0.04
OP1	0	3.9	16.90	92.7	30.22	7.2/8.2	73	-5.80	0.30	0.40	-0.06
	6	3.1	14.48	94.1	29.96	7.2/8.2	72.3	-3.70	0.20	0.20	0.14
OP2	0	4	16.68	93.1	30.14	7.2/8.2	73.5	-5.90	0.30	0.30	-0.03
	6	3.2	14.02	91.8	30.66	7.2/8.2	72.8	-3.70	0.10	0.20	0.02
OP3	0	4	16.40	93.6	30.30	7.2/8.2	74.1	-5.90	0.40	0.30	-0.10
	6	3.0	13.42	96.1	35.52	7.2/8.2	73.3	-3.10	0.30	0.30	-0.10

ISBN: 978-1-61804-195-1

Table 10: Evaluation of impact of the energy farms on the waves in the reference points OP1, OP2 and OP3 for the wave conditions *Hs*=5m, *Tm*=8s, *Dir*=150°.

	WD	Hs (m)	Emax (m^2/Hz/deg)	Dir (deg)	DSPR (deg)	Tm/Tp (s)	Wlen (m)	Px (m^3/s)	Py (m^3/s)	Fx (N/m^2)	Fy (N/m^2)
BP	0	4.5	18.48	145.7	32.26	7.1/8.2	73.0	-3.70	5.50	-0.08	0.09
	6	4.5	18.47	145.9	32.65	7.1/8.2	73.1	-3.70	5.60	-0.08	0.09
OP1	0	3.8	15.29	139.9	27.89	7.2/8.2	72.9	-3.50	4.10	0.39	0.06
	6	3.3	13.96	144.5	29.51	7.2/8.2	71.7	-2.30	3.20	0.37	0.08
OP2	0	3.8	15.57	140.9	28.56	7.2/8.2	73.1	-3.50	4.30	0.36	0.05
	6	3.3	15.61	148.3	29.19	7.2/8.2	72.1	-2.20	3.50	0.40	0.08
OP3	0	3.9	15.87	142.5	28.78	7.2/8.2	73.3	-3.50	4.50	0.34	-0.10
	6	3.5	15.90	151.3	25.04	7.2/8.2	72.9	-2.30	4.10	0.42	0.10

Table 11: Evaluation of impact of the energy farms on the near shore currents in terms of maximum current velocities along the reference lines RL1-RL7 for *Hs*=1m and three different wave directions (30°, 90°,150°). The two configurations (WD0 and WD6) were considered in parallel.

Case study	Line Config.	L1	L2	L3	L4	L5	L6	L7
	WD0	0.93	0.29	0.74	0.33	0.50	0.31	0.49
H1D30	WD6	1.16	0.40	0.75	0.33	0.53	0.30	0.48
	WD0	0.29	0.13	0.23	0.02	0.19	0.08	0.23
H1D90	WD6	0.32	0.15	0.05	0.04	0.25	0.03	0.24
	WD0	0.76	0.25	0.99	0.39	0.74	0.30	0.89
H1D150	WD6	0.73	0.24	0.97	0.38	0.74	0.30	0.89

Table 12: Evaluation of impact of the energy farms on the near shore currents in terms of maximum current velocities along the reference lines RL1-RL7 for *Hs*=3m and three different wave directions (30°, 90°,150°). The two configurations (WD0 and WD6) were considered in parallel.

Case study	Line Config.	L1	L2	L3	L4	L5	L6	L7
	WD0	1.63	0.75	1.20	0.58	0.62	0.69	0.49
H3D30	WD6	1.63	0.75	1.28	0.63	0.64	1.66	0.48
	WD0	0.55	0.31	0.72	0.10	0.22	0.07	0.29
H3D90	WD6	0.68	0.33	0.49	0.21	0.26	0.05	0.30
	WD0	1.04	0.28	1.92	0.74	0.91	0.71	0.94
H3D150	WD6	1.01	0.26	1.89	0.76	0.93	0.36	0.94

Table 13: Evaluation of impact of the energy farms on the near shore currents in terms of maximum current velocities along the reference lines RL1-RL7 for *Hs*=5m and three different wave directions (30°, 90°,150°). The two configurations (WD0 and WD6) were considered in parallel.

Case study	Line Config.	L1	L2	L3	L4	L5	L6	L7
	WD0	1.55	0.70	0.73	0.82	0.50	0.68	0.41
H5D30	WD6	1.55	0.70	1.04	0.86	0.52	0.67	0.40
	WD0	0.34	0.09	1.33	0.50	0.38	0.26	0.43
H5D90	WD6	0.41	0.15	1.25	0.53	0.40	0.26	0.43
	WD0	0.85	0.26	1.98	1.02	0.77	0.32	1.04
H5D150	WD6	0.82	0.24	2.04	1.14	0.77	0.32	1.04

ISBN: 978-1-61804-195-1

The maximum values of the velocities of the near shore currents along the reference lines are illustrated in Fig. 10 for both case studies considered (CS1 and CS2). As the results show, the influence of the wave farm over the near shore currents appear in all the points but in general is not very high. From the analysis of data from the simulations, it has been observed that the most sensitive direction is that normal to the shoreline (90°) and the highest decrease of the current velocityappears in NP3.

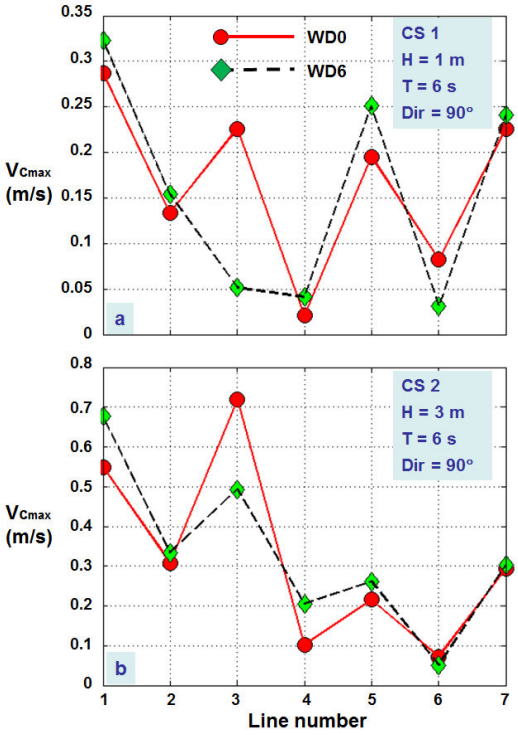

Fig. 10: Evaluation of the impact of the energy farms on the maximum velocities of the near shore currents along the reference lines considered. a) CS1, b) CS2.

An additional issue is related to the assessment of the evolution of the waves after their impact with the body of the WD farm structures. For that, the *Hs* variations have been analyzed along tree reference lines passing through the wave energy farm in different locations, as illustrated in Fig. 11.

The results are presented in Fig. 12 (for Line 1), 13 (for Line 2) and 14 (for Line 3). They all present the evolution of the waves for the two situations WD0 (blue) and WD6 (red).The bathymetric variation along the reference lines is also illustrated in each figure. As it can be seen, the most relevant impact occurs at the reference line 1 in both cases (CS1,CS2) and the lowest is at the reference line 2 due the fact that the line is passing between two devices while in the other two cases the lines pass directly through the body of one WD.

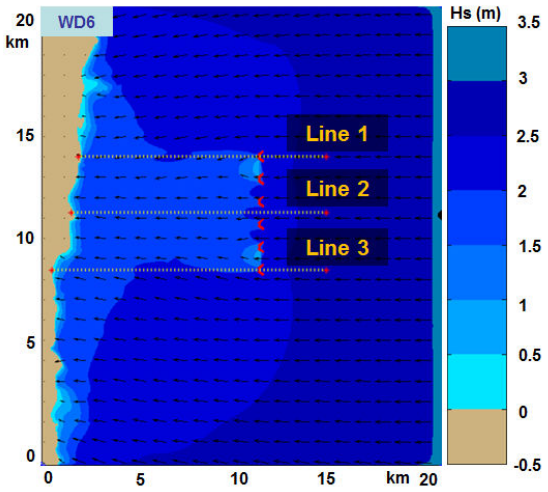

Fig. 11: Evaluation of the impact of the energy farms on the maximum velocities of the near shore currents along the reference lines considered. a) CS1, b) CS2.

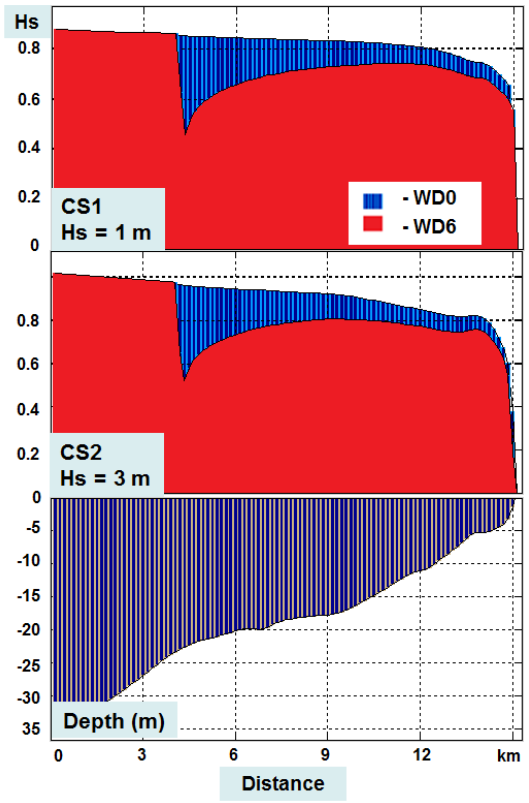

Fig. 12: Hs variation along the reference line 1 without and with WD farm (WD0, WD6) for the two cases considered (CS1, CS2) and the variation of the water depth along the reference line.

ISBN: 978-1-61804-195-1

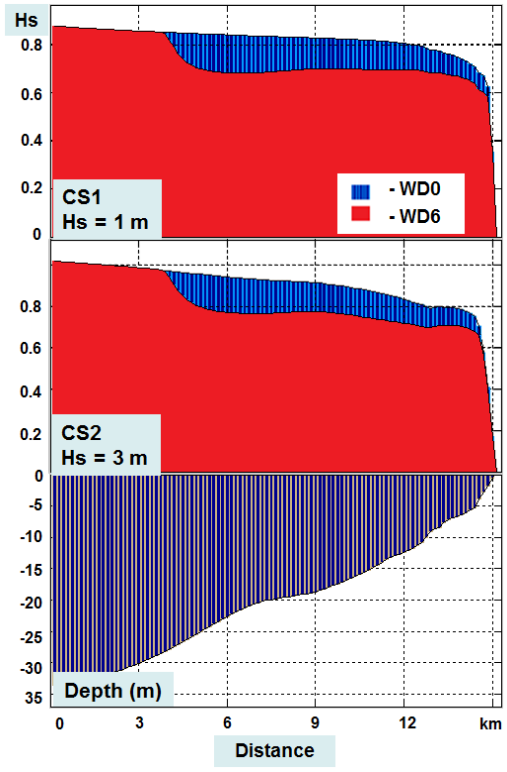

Fig. 13: Hs variation along the reference line 2 without and with WD farm (WD0, WD6) for the two cases considered (CS1,CS2) and the variation of the water depth along the reference line.

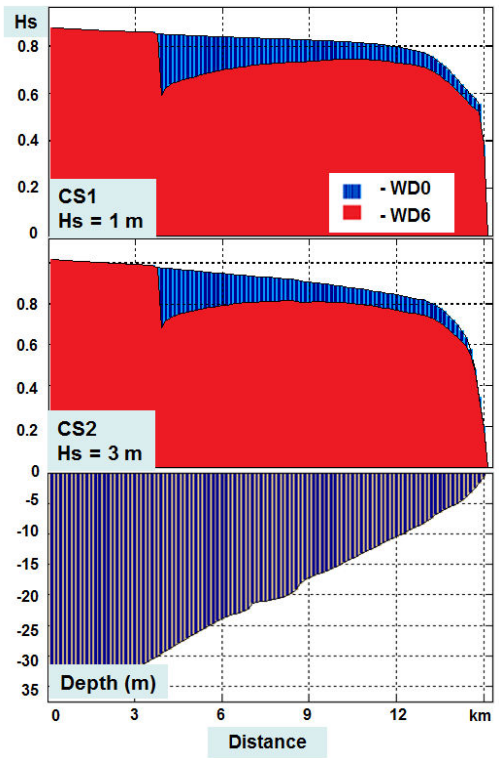

Fig. 14: Hs variation along the reference line 3 without and with WD farm (WD0, WD6) for the two cases considered (CS1,CS2) and the variation of the water depth along the reference line.

Finally, in order to complete the picture, another case study that was analyzed will be presented. This considers the following conditions on the external boundaries: *Hs*=5m, *Tm*=8s, *Dir*=30°. Thus, Fig. 15 illustrates the impact in the geographical space on the wave field and Fig. 16 the evaluation in the spectral space of the impact on the wave field of Wave Dragon farm. For this case study, the maximum values of the velocities of the near shore currents along the reference lines are illustrated in Fig. 17.In such situation, the results of the modeling system indicate that the presence of the energy farm leads this time to an increase of the near shore currents in most places. Finally, Fig. 18 presents the Hs variation along the tree reference lines previously considered, for the two different situations without and with the WEC array.

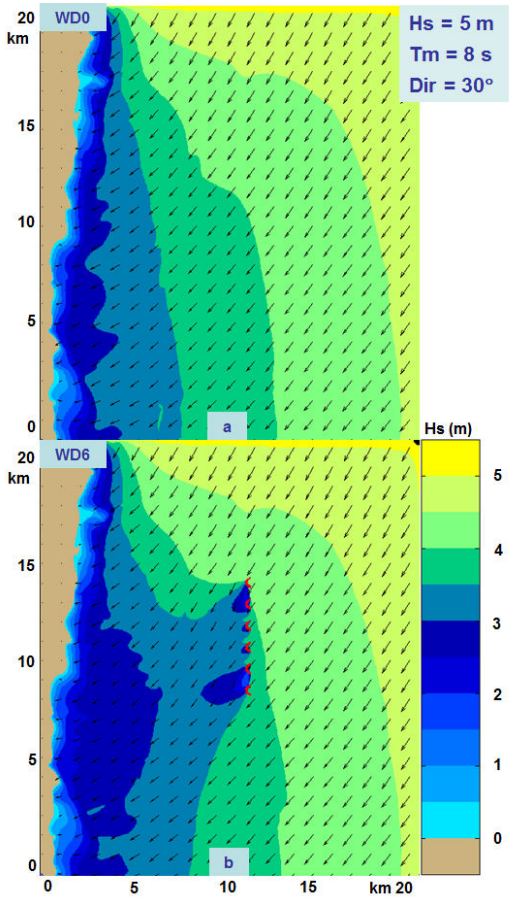

Fig. 15: Hs variation along the reference line 3 without and with WD farm (WD0, WD6) for the two cases considered (CS1,CS2) and the variation of the water depth along the reference line.

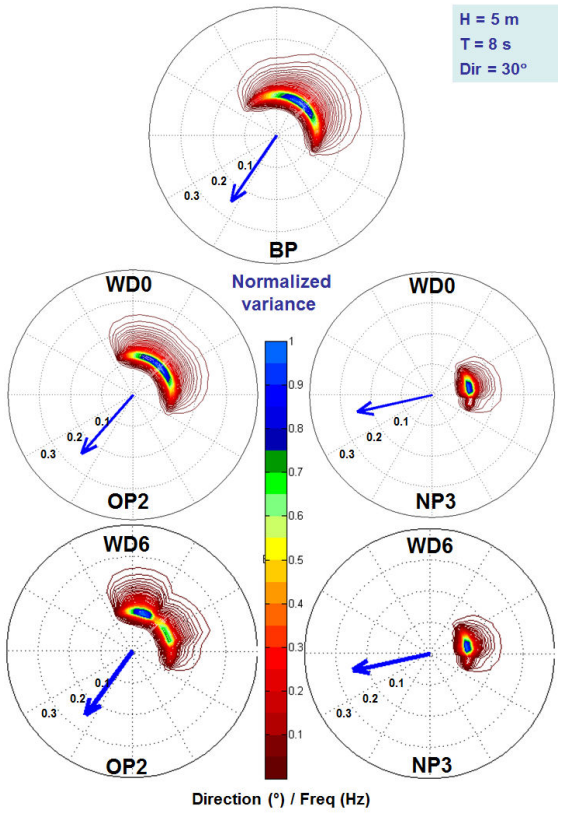

Fig. 16: Evaluation in the spectral space of the impact on the wave field of a wave farm based on Wave Dragon WECs that operates in the target area for an additional case study defined by the parameters *Hs*=5m, *Tm*=8s, *Dir*=30°. a) BP for WD0. b) OP2 for WD0. c) NP3 for WD0, d) OP2 for WD6, e) NP3 for WD6.

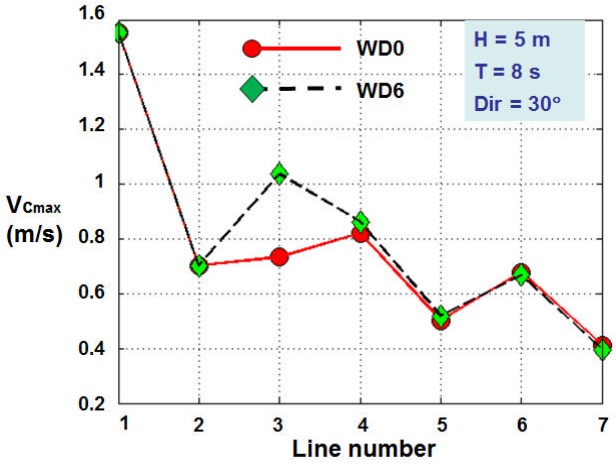

Fig. 17: Evaluation of the impact of the energy farms on the maximum velocities of the near shore currents along the reference lines considered for an additional case study defined by the parameters *Hs*=5m, *Tm*=8s, *Dir*=30°.

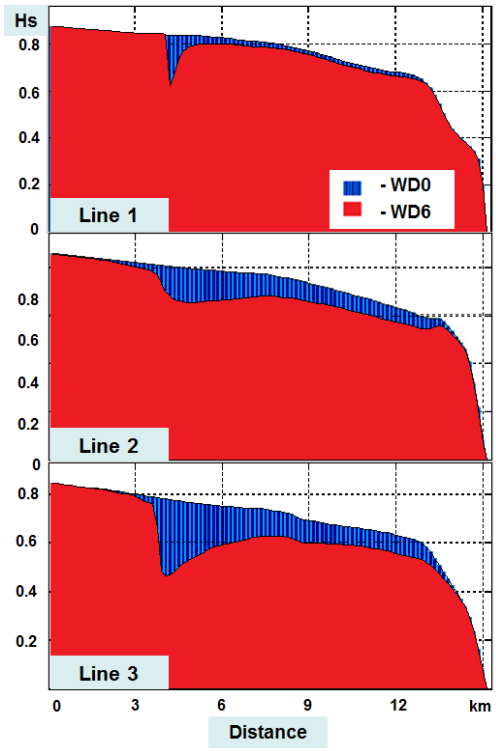

Fig. 18: Hs variation along the tree reference lines without and with the WEC array (WD0 and WD6) for the wave conditions corresponding to the parameters: *Hs*=5m, *Tm*=8s, *Dir*=30°.

5 Concluding remarks

According to the EU requirements, 20% of the electric energy produced in Europe should be provided until 2020 by renewable energy sources. In this connection, the marine environment represents a vast space depositing a huge amount of renewable energy. Nevertheless, the most important problem related with harvesting the energy in marine environment is represented by the high cost of the electric power produced. As regards the wave energy extraction, the most significant step in the direction of reducing the energy cost is represented by the implementation of large WEC arrays. Thus, large scale WEC deployments are expected in the near future and a very important issue related with this perspective is to evaluate correctly the possible coastal impact of these new power plants operating in the near shore. In this context, the present work presents an evaluation of the changes induced in the coastal wave climate by an array of six Wave Dragons. The target area considered is located in the western side of the Black Sea but the

ISBN: 978-1-61804-195-1

methodology can be easily extended to any coastal environment.

As regards the wave transformation, the modeling system considered for these evaluations is based on SWAN spectral model, which represents an adequate framework for accounting the wave changes due to the presence of the energy farm. Evaluations were carried out in both geographical and spectral spaces for various relevant wave patterns. The results show that while immediately after the farm drastically changes occur in the wave fields, these gradually attenuate towards the coast. In order to assess better the changes taking place in the spectral shapes due to the energy farm, transformations of theoretical JONSWAP spectra were followed for each case study considered. The results show that usually the single peaked wave spectra are usually changed by the wave farm in double peaked spectra immediately down wave the farm, but the spectra become again single peaked at the level of the breaking line. This is also due the relatively large distance between the shoreline and the location of the wave farm.

In order to assess better the changes at the level of the shoreline dynamics, the modeling system ISSM that joins SWAN with the 1D surf models was considered. This allowed an evaluation of the long shore currents. The results show that although the near shore waves are not very much affected by the presence of the WD farm, the maximum current velocities may however have significant variations. These variations are more evident at the central near shore points. The results show also that the long shore current velocity is a more sensitive parameter to the presence of the energy farm than the significant wave height.

Since in general the presence of the energy farm leads to slight decreases of the wave conditions its influence at the level of the shoreline dynamics is expected to be rather positive. Nevertheless, a very interesting result coming from the present work is that sometimes the presence of the energy farm may lead locally to enhancements of the long shore current velocity which means that due to the specific features of the site some coastal processes might be also accentuated. The work is still ongoing and larger WEC arrays, both of one and two lines are being considered, which means that more accentuated changes might be expected for such configurations.

Acknowledgment

The work of the first author has been made in the scope of the project SOP HRD - EFICIENT 61445/2009 (Management System for the Fellowships Granted to the PhD Students).

References:

[1] Rusu E. "Wave energy assessments in the Black Sea,"*Journal of Marine Science and Technology*, vol. 14, no. 3, 2009, pp. 359-372.

[2] Rusu L. "Application of numerical models to evaluate oil spills propagation in the coastal environment of the Black Sea,"*Journal of Environmental Engineering and Landscape Management*, vol. 18, no. 4, 2010, pp.288-295.

[3] Rusu L., Ivan A., "Modelling wind waves in the Romanian coastal environment,"*Environmental Engineering and Management Journal*,vol. 9, no. 4, 2010, pp. 547-552.

[4] Rusu, E., Macuta, S.. "Numerical Modelling of Longshore Currents in Marine Environment,"*Environmental Engineering and Management Journal*,vol. 8, no. 1, 2009, pp. 147-151.

[5] Onea F., Rusu E. *"Wind energy assessments along the Black Sea basin,"*Meteorological Applications press,2012.

[6] Babarit, A., Hals, J., Muliawan, M.J., Kurniawan, A., Moan, T., Krokstad, J.. "Numerical benchmarking study of a selection of wave energy converters,"*Renewable Energy,*vol. 41, 2012, pp. 44-63.

[7] Millar, D.L., Smith, H.C.M. Reeve, D.E.. "Modelling analysis of the sensitivity of shoreline change to a wave farm,"*Ocean Engineering,*vol. 34, 2007, pp. 884–901.

[8] Palha, A., Mendes, L., Fortes, C.J., Brito-Melo, A., Sarmento, A.. "The impact of wave energy farms in the shoreline wave climate: Portuguese pilot zone case study using Pelamis energy wave devices,"*Renewable Energy*, vol. 35, 2010, pp. 62–77.

[9] Ponce de Leon, S., Bettencourt, J.H., Kjerstad, N.. "Simulation of irregular waves in an offshore wind farm with a spectral wave model,"*Continental Shelf Research*, vol. 31, no. 15,2011, pp. 1541–1557.

[10] Rusu E. "Modelling of wave-current interactions at the Danube's mouths,"*Journal of Marine Science and Technology,*vol. 15, no. 2, 2010, pp.143-159.

[11] Booij, N., Ris, R. C. and Holthuijsen, L. H.. "A third generation wave model for coastal regions. Part 1: Model description and validation,"*J. Geophys. Res.* vol.104, no. 4,1999, pp. 7649-7666.

[12] Longuet-Higgins, M.S.. "Longshore Currents Generated by Obliquely Incident Sea Waves," I and II, *J. Geophys. Res*., vol. 75,1970, pp. 6778-6801.

[13] Svendsen I.A., Haas, K. and Zhao, Q.. *Quasi-3D Nearshore Circulation Model SHORECIRC*, version 2.0,Center for Applied Coastal Research, University of Delaware, Newark, DE 19716 U.S.A., 2002.

[14] Mettlach, T.R., Earle, M.D. and Hsu, Y.L.. *"Software Design Document for the Navy Standard Surf Model, Version 3.2,"*Naval Research Laboratory, Stennis Space Center, Mississippi,2002, pp. 187.

[15] Conley, D.C., Rusu, E.. *"The Middle Way of Surf Modeling 2006a,"*Proceedings of the 30th International Conference on Coastal Engineering ICCE 2006, 2-9 September, San Diego, USA. Published in World

Scientific Pub Co Inc, Coastal Engineering, 2006, pp. 1053-1065.

[16] *Conley, D.C., Rusu, E.. "Tests of wave shoaling and surf models in a partially enclosed basin,"*Maritime Transportation and Exploitation of Ocean and Coastal Resources,Taylor & Francis Group, London,2006, pp. 1015-1021.

[17] Rusu, E., Conley, D.C., Coelho, E.F.. "A Hybrid Framework for Predicting Waves and Longshore Currents,"*Journal of Marine Systems*, vol. 69, no 1-2, 2008, pp. 59–73.

[18] Rusu, E., Guedes Soares, C.."Validation of Two Wave and Nearshore Current Models,"*Journal of Waterway, Port, Coastal, and Ocean Engineering*, vol. 136, no. 1, 2010, pp. 27-45.

[19] Kofoed JP, Frigaard P, Friis-Madsen E, Sørensen HC. "Prototype testing of the wave energy converter wave dragon,"*Renewable Energy*, vol. 31, 2006, pp. 181–189.